

UC Santa Barbara

UC Santa Barbara Previously Published Works

Title

Seepage Face in Steady-State Groundwater Flow between Two Water Bodies

Permalink

<https://escholarship.org/uc/item/7tp5z3g2>

Journal

Journal of Hydrologic Engineering, 25(9)

ISSN

1084-0699

Author

Loáiciga, Hugo A

Publication Date

2020-09-01

DOI

10.1061/(asce)he.1943-5584.0001997

Peer reviewed



Seepage Face in Steady-State Groundwater Flow between Two Water Bodies

Hugo A. Loáiciga, Dist.M.ASCE¹

Abstract: An implicit solution determining the seepage-face dimension formed in steady-state flow through an aquifer connecting two water bodies is achieved based on the Dupuit assumption and conservation-of-flow-rate considerations. The aquifer features sloping upstream and downstream boundaries. The solution approach presented here yields the seepage-face dimension, the flow rate through the aquifer, the geometry of the phreatic surface, and travel times along streamlines. The Dupuit-based groundwater flow estimates compare well with numerical solutions calculated for the exact groundwater flow problem. DOI: 10.1061/(ASCE)HE.1943-5584.0001997. © 2020 American Society of Civil Engineers.

Author keywords: Seepage face; Dupuit assumption; Phreatic surface; Steady state; Groundwater flow.

Introduction

Fig. 1 depicts groundwater flow established between two water bodies of constant levels h_1 (upstream water body) and h_2 (downstream water body). The situation displayed in Fig. 1 may involve two natural water bodies, such as lakes or groundwater flow established through an embankment, levee, or earth dam. On the downstream slope surface (EI) of the flow system shown in Fig. 1 there exists a slope segment (FG) where groundwater discharges from the aquifer and flows overland and downslope toward the downstream water body. The slope segment FG is called the seepage face, which has an unknown vertical dimension, herein denoted by a . Empirical evidence confirms the existence of the seepage face, and there are theoretical reasons requiring the existence of a seepage face in the type of groundwater flow depicted in Fig. 1 (e.g., Bear 1972, p. 260). The case in which the slope angles α and β equal 90° and the seepage face is neglected (i.e., $a = 0$) in Fig. 1 represents a classic case of steady-state groundwater flow (i.e., the so-called two-lake problem) for which there are closed-form solutions for the flow rate between the two water bodies and for the shape of the phreatic surface (Line BF in Fig. 1) under the Dupuit assumption, i.e., assuming groundwater flow is essentially horizontal and equipotential surfaces (i.e., surfaces on which the hydraulic head is constant) are nearly vertical (e.g., Bear 1979, p. 76). The Dupuit assumption is widely used in the solution of steady and transient groundwater-hydraulics problems (e.g., Ritzi and Bobeck 2008). The Dupuit assumption is perhaps the most powerful, and possibly the only simple, tool to solve unconfined groundwater flow analytically. The largest deviation of the flow regime from the Dupuit assumption occurs along Boundaries AB and FG in Fig. 1.

Let q denote the rate of groundwater flow moving from the upstream water body to the downstream water body. The flow rate q is per unit width of aquifer normal to the plane of Fig. 1. In addition, let $h(x)$ and K denote respectively the hydraulic head a distance x from the origin A and the (saturated) hydraulic conductivity of the

aquifer's soil. The solutions for the classic two-lake groundwater problem are as follows (e.g., Fetter 2001):

$$q = K \frac{h_1^2 - h_2^2}{2L} \quad \alpha = \beta = 90^\circ; a = 0 \quad (1)$$

$$h(x) = \sqrt{h_1^2 - \frac{[h_1^2 - (h_2)^2] \cdot x}{L}} \quad \alpha = \beta = 90^\circ; a = 0; 0 \leq x \leq L \quad (2)$$

where $L = w$ if $\beta = 90^\circ$; w = width separating the two slopes' crowns; and α and β = angles of upstream and downstream slopes, respectively. Eq. (1) was first reported by Dupuit (1863). Eq. (2) expresses the elevation of the phreatic surface under the Dupuit assumption. It is noteworthy that the flow rate q given in Eq. (1) is constant between the upstream and the downstream water bodies. Yet the seepage velocity (or average linear velocity) of groundwater varies with position x between the two water bodies. The travel time (t_L) of groundwater between the two water bodies when $\alpha = \beta = 90^\circ$ is obtained by (1) deriving the seepage velocity (v) from the hydraulic gradient defined by the spatial derivative of the equation for the phreatic surface [Eq. (2)], the hydraulic conductivity, and the aquifer porosity (n), i.e., $v = -K(dh/dx)/n$, and (2) integrating by separation of variables the formula $v^{-1} dx = dt$. The result for the travel time is as follows:

$$t_L = \frac{4}{3} \cdot \frac{nL^2}{K} \cdot \frac{h_1^3 - h_2^3}{(h_1^2 - h_2^2)^2} \quad \alpha = \beta = 90^\circ; a = 0 \quad (3)$$

Eqs. (1)–(3) provide useful information about the rate of groundwater flow, the position of the phreatic surface, and the travel time between water bodies, respectively, when the upstream and downstream aquifer boundaries are vertical and neglecting the seepage face. Vertical aquifer boundaries are rare in practice, even in constructed porous media, perhaps occurring naturally only when the aquifer is made of highly cohesive soil or fractured rock. Polubarinova-Kochina and de Wiest (1962) reported a method to calculate the seepage face of the two-lake problem with vertical lateral boundaries and showed that Eq. (1) also gives the groundwater flow between the lakes when (1) there is a seepage face and $\alpha = \beta = 90^\circ$ and (2) there are vertical and horizontal hydraulic gradients [i.e., without resorting to the Dupuit assumption;

¹Professor, Dept. of Geography, Univ. of California, Santa Barbara 93106, California. Email: hloaiciga@ucsb.edu

Note. This manuscript was submitted on March 28, 2019; approved on May 19, 2020; published online on July 8, 2020. Discussion period open until December 8, 2020; separate discussions must be submitted for individual papers. This technical note is part of the *Journal of Hydrologic Engineering*, © ASCE, ISSN 1084-0699.

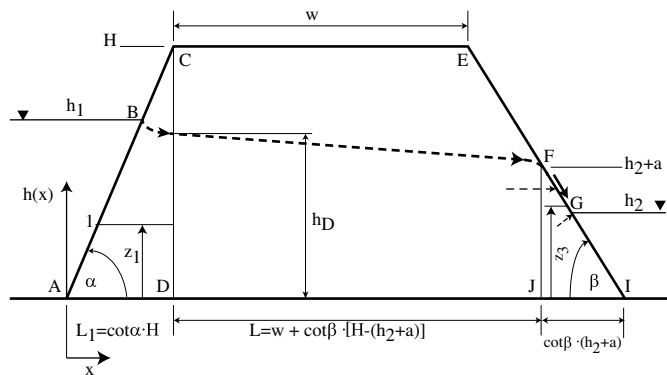


Fig. 1. Geometry of flow system showing parameters; elevation view not drawn to scale.

see Eq. (9.10), Chapter VII, of Polubarinova-Kochina and de Wiest (1962)]. The latter method does not solve the case of sloping upstream and downstream aquifer boundaries; nor does the hodograph method employed to find analytical solutions to some specialized groundwater flow problems (Polubarinova-Kochina and de Wiest 1962). Chapuis and Chenaf (2007) presented a numerical analysis of and predictive equations for the seepage face at the borehole of a fully penetrating well withdrawing groundwater from an ideal unconfined aquifer in steady state. Rushton and Youngs (2010) reported solutions to the vertical-boundary, two-lake problem with recharge onto the phreatic surface. The latter authors relied on numerical solutions to the 2D Laplace equation without recourse to the Dupuit assumption. This work presents solutions to the groundwater flow problem between two water bodies in the general case where the upstream and downstream aquifer boundaries are sloping, that is, when $0^\circ < \alpha, \beta < 90^\circ$, considering the presence of a seepage face, and relying on the Dupuit assumption. The solutions yield the magnitude of the seepage face, the flow rate through the aquifer, the position of the phreatic surface, and the travel times through the aquifer under the stated conditions of groundwater flow. This work also presents a comparison of its analytical results with numerical simulations of the exact groundwater flow problem corresponding to the aquifer geometry displayed in Fig. 1. Besides this work's theoretical contribution, there are practical applications of the formulas herein introduced. The rate of groundwater flow is of interest from the perspective of water balance in the type of flow system depicted in Fig. 1. The position of the phreatic surface is pertinent to the planning and execution of recharge operations (Bouwer 2002) and in the analysis of slope stability (Duncan et al. 2014; Loáiciga 2015). The travel time between the two water bodies is relevant to the temporal analysis of advective transport of dissolved matter.

Methodology

Groundwater Flow and the Seepage Face (General Case $0^\circ < \alpha, \beta < 90^\circ$; $a > 0$)

The central region CEFJD in Fig. 1 is equivalent to a flow system in which the upstream and downstream aquifer boundaries are vertical, in which case the solutions of the flow through the aquifer and the phreatic surface's position are known. Therefore, Eqs. (1) and (2) are extended to represent respectively the flow rate (q) through this central region and the elevation of the phreatic surface [$h(x)$] as follows:

$$q = K \frac{h_D^2 - (h_2 + a)^2}{2L} \quad (4)$$

in which $L = w + \cot \beta \cdot [H - (h_2 + a)]$, and h_D represents the (unknown) elevation of the phreatic surface at $L_1 = \cot \alpha \cdot H$

$$h(x) = \sqrt{h_D^2 - \frac{[h_D^2 - (h_2 + a)^2] \cdot (x - L_1)}{L}} \quad L_1 \leq x \leq L + L_1 \quad (5)$$

The flow rate Eq. (4) contains three unknowns, namely, a , h_D , and q . Therefore, two additional equations are needed to solve for the three unknowns. The groundwater flow moving through the triangular Regions ACD and FIJ shown in Fig. 1 must also equal the flow rate q given by Eq. (5) under steady state. The equations describing groundwater flow through the latter two regions provide the required additional equations. Regions ACD and FIJ encompass the upstream and downstream lake boundaries. They must be chosen as done in Fig. 1 to provide the necessary flow equations to solve the groundwater flow problem between two lakes with sloping, submerged boundaries. Careful consideration of the choice of flow regions must be made in each groundwater flow situation, as required by the method of fragments (e.g., Harr 1962). Using the Dupuit assumption of nearly horizontal streamlines, in the triangular Region ACD a streamline segment is seen starting at Point 1 with elevation z_1 and ending on the vertical equipotential surface whose hydraulic head equals h_D defines a hydraulic gradient equal to

$$i_1 = \frac{h_1 - h_D}{\cot \alpha \cdot (H - z_1)} \quad (6)$$

The groundwater flow rate moving through the triangular Region ACD in Fig. 1 is obtained by applying Darcy's law to obtain a differential flow rate $dq = K \cdot i_1 \cdot dz_1$ and integrating from 0 through h_D to obtain the flow rate q as follows:

$$q = K \cdot \frac{h_1 - h_D}{\cot \alpha} \cdot \ln \left(\frac{H}{H - h_D} \right) \quad (7)$$

The third needed equation is obtained by analyzing the groundwater flow rate moving through the triangular Region FIJ shown in Fig. 1. A streamline intersecting the equipotential Surface FJ at an elevation z_3 (where the hydraulic head equals $h_2 + a$) and ending on the seepage Face FG (where the hydraulic head equals z_3) defines a hydraulic gradient equal to (using the Dupuit assumption)

$$i_{FG} = \frac{h_2 + a - z_3}{\cot \beta \cdot (h_2 + a - z_3)} = \tan \beta \quad (8)$$

Likewise, a streamline intersecting the equipotential Surface FJ at an elevation z_3 (with hydraulic head equal to $h_2 + a$) and ending on the Slope Segment GI of the downstream slope (with a hydraulic head h_2) defines a hydraulic gradient equal to

$$i_{GI} = \frac{a}{\cot \beta \cdot (h_2 + a - z_3)} \quad (9)$$

The hydraulic gradients i_{FG} and i_{GI} define differential flow rates $K \cdot i_{FG} \cdot dz_3$ and $K \cdot i_{GI} \cdot dz_3$, respectively. Integrating the former and the latter differential flow rates between h_2 and $h_2 + a$ and between 0 and h_2 , respectively, and adding the resulting expressions yields the groundwater flow rate moving through the triangular Region FIJ:

$$q = K \cdot \frac{a}{\cot \beta} \cdot \left[1 + \ln \left(\frac{h_2 + a}{a} \right) \right] \quad (10)$$

Eqs. (4), (7), and (10) provide the three equations involving the flow system's three unknowns. They must be solved jointly, as explained in what follows. The case of a vertical upstream boundary ($\alpha = 90^\circ$) is solved using Eq. (4) with $h_D = h_1$ and Eq. (10). The case of a vertical downstream boundary ($\beta = 90^\circ$) is not solvable with this paper's methodology, although one can let $\beta \rightarrow 90^\circ$ to approximate the seepage-face dimension a in this instance.

Travel Times in the General Case $0^\circ < \alpha, \beta < 90^\circ$; $a > 0$

Travel times in the general case $0^\circ < \alpha, \beta < 90^\circ$; $a > 0$

The travel time along the streamline starting at Point 1 and elevation $z \leq h_2$ on the slope Segment AB of the upstream Slope AC is the sum of the travel times through Regions ACD (t_1), CEFJD (t_L), and FIJ exiting between G and I (t_{GI} ; see Fig. 1). The travel times through Regions ACD and FIJ are calculated by dividing the travel distance (which is approximately horizontal under the Dupuit assumption) by the seepage velocity in each region. The travel time through Region CEFJD must be obtained by integrating the inverse of the seepage velocity over the flow distance. Recalling the expression for t_L in Eq. (3) and the hydraulic gradients i_1 and i_{GI} expressed by Eqs. (6) and (9), respectively, the travel time between the two water bodies (t_{12}) is given by the following expression:

$$t_{12}(z) = \frac{n}{K} \frac{[\cot \alpha \cdot (H - z_1)]^2}{h_1 - h_D} + \frac{4}{3} \cdot \frac{nL^2}{K} \cdot \frac{h_D^3 - (h_2 + a)^3}{(h_D^2 - (h_2 + a)^2)^2} + \frac{n}{K} \frac{[\cot \beta \cdot (h_2 + a - z_3)]^2}{a} \quad (11)$$

in which $0 \leq z_1 = z_3 \leq h_2$. The longest travel distance occurs along the basal Boundary AI and equals $L_1 + L + (h_2 + a) \cdot \cot \beta$; the travel time along the basal boundary is given by Eq. (11) with $z_1, z_3 = 0$.

The travel time along a streamline starting at Point 1 and elevation $h_2 \leq z_1 \leq h_1$ on the slope Segment AB of the upstream Slope AC and emerging on the slope Segment FG of the downstream boundary at elevation $h_2 \leq z_3 \leq h_2 + a$ is the sum of the travel times through Regions ACD (t_1), CEFJD (t_L), and FIJ exiting between F and G (t_{FG} ; see Fig. 1). The procedure to calculate the travel time between the two water bodies is similar to that leading to Eq. (11). The result is as follows:

$$t_{12}(z) = \frac{n}{K} \frac{[\cot \alpha \cdot (H - z_1)]^2}{h_1 - h_D} + \frac{4}{3} \cdot \frac{nL^2}{K} \cdot \frac{h_D^3 - (h_2 + a)^3}{(h_D^2 - (h_2 + a)^2)^2} + \frac{n}{K} (\cot \beta)^2 \cdot (h_2 + a - z_3) \quad (12)$$

in which z_1 and z_3 represent the extremities of a streamline. The travel time along the phreatic Surface BF is given by Eq. (12) with $z_1 = h_1$ and $z_3 = h_2 + a$.

Solution Approach

Eqs. (4), (7), and (10) provide the three equations needed to solve for the vertical extent of the seepage face (a), the groundwater flow rate between the two water bodies (q), and the hydraulic head h_D at location L_1 . The three equations are nonlinear on the unknowns, which prevents a closed-form solution; yet a solution can be achieved by solving a sequence of implicit equations. Equating Eqs. (4) and (10) and solving for h_D as a function of a produces the following result, denoted by $h_D[a]$:

$$h_D[a] = \left\{ (h_2 + a)^2 + \frac{2aL}{\cot \beta} \cdot \left[1 + \ln \left(\frac{h_2 + a}{a} \right) \right] \right\}^{\frac{1}{2}} \quad (13)$$

The expression $h_D[a]$ given by Eq. (13) replaces h_D in Eq. (7), and the resulting expression is equated with Eq. (10) to render the following implicit equation for the seepage-face dimension a :

$$\frac{h_1 - h_D[a]}{\cot \alpha} \cdot \ln \left(\frac{H}{H - h_D[a]} \right) = \frac{a}{\cot \beta} \cdot \left[1 + \ln \left(\frac{h_2 + a}{a} \right) \right] \quad (14)$$

Eq. (14) must be solved numerically to yield a . Double-precision calculation must be implemented to achieve equality of the left- and right-hand sides of Eq. (14) with sufficient precision. The hydraulic head h_D is calculated using Eq. (13) once a is determined from Eq. (14). It is noteworthy that the solutions of Eqs. (13) and (14) do not involve the hydraulic conductivity K . The groundwater flow rate is determined with Eqs. (4), (7), or (10). These three equations must produce the same result for q if the solution is correctly calculated. The travel time t_{12} is calculated with either Eqs. (11) or (12). The case of vertical upstream slope ($\alpha = 90^\circ$) and downstream head $h_2 = 0$ produces a closed-form solution for the groundwater flow and the seepage face by equating Eq. (4) with $h_D = h_1$ and $h_2 = 0$ to Eq. (10) with $h_2 = 0$. The results are as follows:

$$q = Ka \tan \beta \quad (15)$$

$$a = -L \tan \beta + \sqrt{L^2 \tan^2 \beta + h_1^2} \quad (16)$$

which are applicable for $0^\circ < \beta < 90^\circ$. Casagrande (1937) reported alternative and approximate solutions to Eqs. (15) and (16). Other approximate solutions to the seepage-face problem considered in this work were proposed in the early 1900s, with pertinent references found in Casagrande (1937). Those approximate solutions do not consider the exact flow transition between Regions ACD and CEFJD, as done in this work.

Formulation of Two-Lake Problem for Numerical Solution

The groundwater regime that takes place in an aquifer depicted by Fig. 1 does not have flow components along the dimension perpendicular to the figure's plane (i.e., there is plane flow in this instance). Therefore, the governing two-dimensional (2D) groundwater flow equation in an aquifer setting as shown in Fig. 1 is given by Laplace's equation:

$$\frac{\partial^2 h(x, z)}{\partial x^2} + \frac{\partial^2 h(x, z)}{\partial z^2} = 0 \quad (17)$$

The boundary conditions associated with Eqs. (17) are as follows:

Upstream constant head:

$$h(x, z) = h_1 \quad (18)$$

on boundary AC, $z = \tan \alpha \cdot x$; $0 \leq x \leq h_1 \cot \alpha$; $0 \leq z \leq h_1$.

No flow across the lower boundary of the flow region:

$$\frac{\partial h}{\partial z} = 0 \quad (19)$$

on boundary AI, $0 \leq x \leq H \cdot (\cot \alpha + \cot \beta) + w$.

The phreatic surface constitutes the upper boundary of the flow region:

$$h(x, z_f) = z_f(x) \quad (20)$$

on the phreatic surface BF, $\cot \alpha \cdot h_1 \leq x \leq \cot \alpha \cdot h_1 + L$, where $z_f(x)$ represents the variable and unknown elevation of the phreatic surface.

Variable head along the seepage face FG:

$$h(x, z) = z \quad (21)$$

the formula for the FG boundary is $z = h_2 + a + \tan \beta \cdot (L_1 + L) - \tan \beta \cdot x$, where

$$L_1 + L \leq x \leq L_1 + L + a \cot \beta; \quad h_2 \leq z \leq h_2 + a$$

Downstream constant head:

$$h(x, z) = h_2 \quad (22)$$

the formula for the GI boundary is $z = h_2 + a + \tan \beta \cdot (L_1 + L) - \tan \beta \cdot x$, where

$$L_1 + L + a \cot \beta \leq x \leq L_1 + L + (h_2 + a) \cot \beta; \quad 0 \leq z \leq h_2$$

The problem defined by Eqs. (17)–(22) does not have an analytical solution. It must be solved numerically. The specification of the seepage-face boundary condition given by Eq. (21) introduces a dilemma of circular logic: it depends on the seepage-face variable a , which is unknown; to determine a , one must solve for the position of the phreatic surface, which requires knowledge of a . Numerical models, such as the well-known MODFLOW software, can solve Eqs. (17)–(22) ignoring the seepage face. In that case, the position of the phreatic surface is determined by an iterative scheme. The results section presents a comparison of groundwater flow calculations obtained with the Waterloo Hydrogeologic Visual Modflow Flex model and with this work's analytical solutions. The procedure followed to construct the comparison relies on (1) calculating the seepage-face dimension a with this paper's method, (2) solving the groundwater flow problem given by Eqs. (17)–(22) numerically after specifying the seepage-face dimension a based on the results from (1), and (3) comparing the numerically obtained flow rate with the flow rate calculated using this paper's method. This comparison reveals the extent to which the flow rates calculated with the numerical model differ from those obtained under the Dupuit assumption and using this paper's method. The comparison also provides insight into the difference between the Dupuit-based seepage-face dimension and its value considering horizontal and vertical hydraulic gradients. It is noteworthy that the seepage-face dimension a cannot be obtained with numerical models.

Results

Dupuit-Based Seepage Face and Groundwater Flow Calculations

The seepage dimension, flow rate, shape of the phreatic surface, and travel time were calculated for selected combination of the water levels h_1 and h_2 . The downstream water level (h_2) was varied between 10 and 29 m while setting the upstream water level constant ($h_1 = 30$ m). Other hydraulic parameters equaled $\alpha = \beta = 26.5^\circ$ (one unit of vertical rise to two units of horizontal distance), $H = 32$ m, $K = 1$ m/day, $n = 0.30$, and $w = 500$ m.

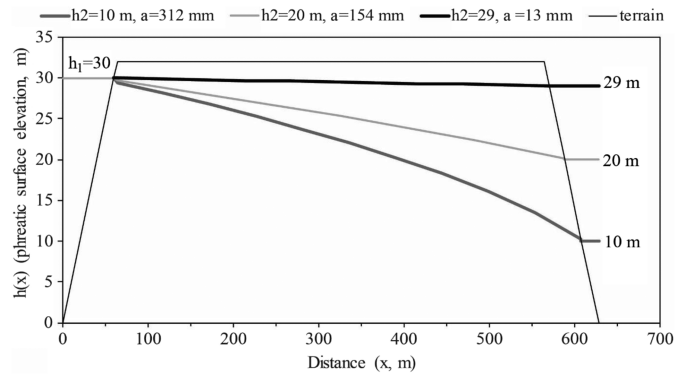


Fig. 2. Variation of phreatic surface for water levels h_1 and h_2 (not drawn to scale).

Fig. 2 depicts the phreatic surface calculated for downstream water elevations $h_2 = 29, 20,$ and 10 m, for which the calculated seepage-face dimension a equaled 13, 154, and 312 mm, respectively. A prominent feature arising from the calculation of the seepage-face dimension a is its relatively small magnitude, which varies from 13 to 312 mm as the downstream water level ranges between 29 and 10 m.

A second set of calculations involved the flow rate and travel time corresponding to several combinations of upstream and downstream water levels. The downstream water level (h_2) was once more varied between 10 and 29 m while setting the upstream water level constant ($h_1 = 30$ m). Other hydraulic parameters were identical to those used in preparing Fig. 2. The hydraulic gradient defined by the boundaries of the phreatic surface was calculated once the seepage dimension was determined corresponding to several combinations of water levels h_1 and h_2 . The hydraulic gradient in this instance is defined as the total drop in elevation along the phreatic surface divided by the horizontal distance separating the upstream and downstream boundaries of the phreatic surface:

$$i = \frac{h_1 - (h_2 + a)}{(H - h_1) \cdot \cot \alpha + L} \quad (23)$$

Fig. 3 depicts the calculated variation of the travel time along the phreatic surface and the flow rate with respect to the hydraulic gradient. The flow rate was calculated considering the seepage face (1) with Eqs. (4), (7), or (10) and (2) neglecting the seepage

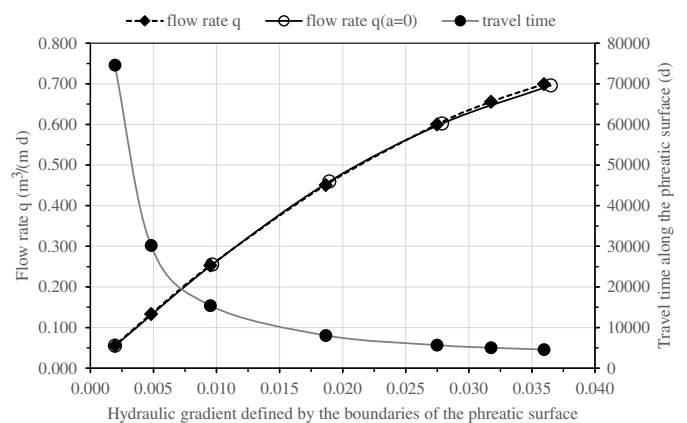


Fig. 3. Variation of groundwater flow rate and travel time with hydraulic gradient.

Table 1. Results obtained with Dupuit-based and numerical methods

h_1 (m)	h_2 (m)	a (mm)	q (this paper's method) ($\text{m}^3/\text{m} \cdot \text{d}$)	q (visual modflow flex) ($\text{m}^3/\text{m} \cdot \text{day}$)
30	10	312	0.70	0.68
30	20	154	0.45	0.43
30	29	13	0.06	0.05

face with Eq. (4) (setting $a = 0$) or Eq. (7). In the latter case, the unknown h_D is solved for by equating Eq. (4) (with $a = 0$) to Eq. (7) and finding the h_D that achieves equality. The flow rates considering and without considering the seepage are nearly identical over the entire range of the hydraulic gradient, as depicted in Fig. 3. It is seen in Fig. 3 that the flow rate and the travel time vary nonlinearly with a changing hydraulic gradient. The travel time in particular increases rapidly as the hydraulic gradient falls below 10/1,000.

Numerical Solutions

The Visual Modflow Flex model was implemented by constructing a finite-difference grid for Region AHEI depicted in Fig. 1. The grid had cells of size 25 cm (horizontal coordinate) \times 10 cm (vertical coordinate). The direction perpendicular to the plane of the flow region was assigned a thickness equal to 100 cm. The seepage-face dimension a was calculated using the Dupuit-based method herein developed and input as a known variable to the numerical model. The hydraulic head conditions given by Eqs. (18), (21), and (22) were specified in the model by assigning pertinent numerical values with the graphical user interface of the boundary module of Visual Modflow Flex. The numerical model was run specifying unconfined conditions, which solves for the phreatic surface in terms of the values of the hydraulic head on the uppermost cells of the region where flow occurs. The no-flow boundary [Eq. (19)] is automatically generated by the numerical model by the geometry of the finite-difference grid.

Table 1 lists the comparison of flow rates obtained with this paper method's and with Visual Modflow Flex. The aquifer geometry and hydraulic characteristics are the same as those used to construct Figs. 2 and 3.

The results in Table 1 indicate the numerically calculated flow is slightly smaller than the flow calculated with this paper's method based on the Dupuit assumption. This suggests that achieving equality of flows by the two methods herein applied would require a slightly larger hydraulic gradient (i.e., h_2 is smaller for a given h_1) in the numerical simulation than that driving groundwater flow under the Dupuit assumption. This implies the seepage-face dimension must be slightly larger under 2D flow conditions than that calculated under the Dupuit assumption. The larger Dupuit-based flow may be explained by the fact that it relies on the assumption of nearly horizontal flow conditions, which creates more efficient water transport under given geometric conditions compared with the actual flow driven by horizontal and vertical gradients.

Conclusion

This paper has presented a methodology to calculate the seepage-face dimension, flow rate, and travel times through an aquifer with sloping boundaries connecting two water bodies with constant water levels and featuring a seepage face on the downstream boundary. The results for the seepage-face dimension indicate it is relatively small over a wide range of the hydraulic gradient driving flow in the aquifer under the Dupuit assumption. The flow rate and travel times vary considerably with the changing hydraulic gradient. A comparison of flow rates calculated under the Dupuit assumption and with a numerical model, which better represents the actual groundwater flow regime, indicates the numerically calculated groundwater flow is slightly smaller than that calculated under the Dupuit assumption. The closeness of the calculated Dupuit-based and numerically based flows demonstrates the robustness of the Dupuit assumption as a tool for solving the type of problems considered in this work.

Data Availability Statement

This paper's results were calculated with an Excel spreadsheet, which is available upon request.

References

- Bear, J. 1972. *Dynamics of fluids in porous media*. New York: Dover.
- Bear, J. 1979. *Hydraulics of groundwater*. New York: McGraw-Hill.
- Bouwer, H. 2002. "Artificial recharge of groundwater: Hydrogeology and engineering." *Hydrogeol. J.* 10 (1): 121–142. <https://doi.org/10.1007/s10040-001-0182-4>.
- Casagrande, A. 1937. "Seepage through dams." *J. N. Engl. Water Works Assoc.* 51 (2): 131–172.
- Chenaf, D., and R. P. Chapuis. 2007. "Seepage faces height, water table position, and well efficiency at steady state." *Ground Water* 45 (2): 168–177. <https://doi.org/10.1111/j.1745-6584.2006.00277.x>.
- Duncan, J. M., S. G. Wright, and T. L. Brandon. 2014. *Soil strength and slope stability*. Hoboken, NJ: Wiley.
- Dupuit, J. 1863. *Études théoriques et pratiques sur le mouvement des eaux*. Paris: Dunod.
- Fetter, C. W. 2001. *Applied hydrogeology*. Upper Saddle River, NJ: Prentice Hall.
- Harr, M. E. 1962. *Groundwater and seepage*. New York: McGraw-Hill.
- Loáiciga, H. A. 2015. "Groundwater and earthquakes: Screening analyses for slope stability." *Eng. Geol.* 193 (Jul): 276–287. <https://doi.org/10.1016/j.enggeo.2015.04.027>.
- Polubarinova-Kochina, P. Y., and R. de Wiest. 1962. *Theory of groundwater movement*. Princeton, NJ: Princeton University Press.
- Ritzi, R. W., and P. Bobeck. 2008. "Comprehensive principles of quantitative hydrogeology established by Darcy (1856) and Dupuit (1857)." *Water Resour. Res.* 44 (10): W10402. <https://doi.org/10.1029/2008WR007002>.
- Rushton, K. R., and E. G. Youngs. 2010. "Drainage of recharge to symmetrically located downstream boundaries with special reference to seepage faces." *J. Hydrol.* 380 (1–2): 94–103. <https://doi.org/10.1016/j.jhydrol.2009.10.026>.